Build Simul
https://doi.org/10.1007/s12273-025-1348-1

A comprehensive framework for building flexibility assessment: RC-Mapping modeling, flexibility quantification, and uncertainty analysis

Huilong Wang[1], Xiyin Weng[1], Yongjun Sun[2] (✉), Pengyuan Shen[3] (✉)

1. State Key Laboratory of Intelligent Geotechnics and Tunnelling (Shenzhen University), Shenzhen 518060, China
2. Department of Architecture and Civil Engineering, City University of Hong Kong, Hong Kong, China
3. Institute of Future Human Habitats, Shenzhen International Graduate School, Tsinghua University, Shenzhen, China

Abstract

The increasing integration of renewable energy sources highlights the urgent need for grid flexibility, with buildings serving as key controllable loads. In this context, accurately quantifying building flexibility is essential for enabling effective demand-side management and ensuring reliable grid operations. However, several challenges hinder this quantification. To address these issues, this study proposes a comprehensive flexibility quantification framework. First, a novel RC-Mapping model incorporating an Enumerate-Comparison Method is proposed. The RC-Mapping model can capture the thermal behavior of both the building and the air conditioning system, while the Enumerate-Comparison Method can initialize state parameters in the RC-Mapping model. Compared with the conventional approach, as validated by the experiment, the proposed method can substantially improve RMSE for indoor temperature prediction from 0.542 °C to 0.266 °C, and the MAPE for flexibility quantification from 27.58% to 10.98%. Second, the study introduces the power reduction-duration curve and temperature variation curves to characterize flexibility from both grid and building perspectives. Specifically, based on the analysis of the power reduction-duration curve, this study provides a systematic analysis of four sources of flexibility and their underlying mechanisms, including the thermal storage of the building, the thermal storage of the HVAC system, the increase of coefficient of performance (COP), and the reduction in cooling load. Finally, the study investigates the impact of uncertainties in COP and internal heat gains on flexibility quantification. According to the result, it is recommended to slightly underestimate the COP and overestimate the internal heat gain schedule to improve the accuracy of flexibility quantification.

Keywords

flexibility quantification
RC-Mapping model
demand response
HVAC system

Article History

Received: 27 June 2025
Revised: 27 July 2025
Accepted: 08 August 2025

1 Introduction

In response to the global energy crisis and the pursuit of carbon neutrality goals, countries are accelerating the development and utilization of renewable energy sources (Ding et al. 2022). However, as the penetration of renewable energy into power systems continues to increase (Luo et al. 2023b), the intermittent and uncertain nature of these energy sources is posing significant challenges to the stability of power systems (Arteconi et al. 2019). In addition, the growing frequency of extreme weather events increases peak load pressures on power systems, necessitating greater system flexibility (Li et al. 2022). Traditionally, peak power demand has been addressed by constructing new power plants (Klein et al. 2017). However, this approach results in increased energy costs and significantly reduced annual utilization of generators, reducing its viability in smart grid applications (Rao et al. 2023; Wang et al. 2023).

In this context, the rapid development of grid interaction technologies has created new opportunities for the utilization

E-mail: yongjsun@cityu.edu.hk (Yongjun Sun); pengyuan_pub@163.com (Pengyuan Shen)

List of symbols

ass	assumption
C	thermal capacitance (J/K)
cal	calculation
COP	coefficient of performance
DR	demand response
F	flexibility
GA	genetic algorithm
h	the number of hour
HVAC	heating, ventilation, and air conditioning
J	objective function
MAPE	mean absolute percentage error
MPE	mean percentage error
P	power (W)
ΔP	power reduction (W)
R	thermal resistance (K/W)
RMSE	root mean squared error
schedule	internal heat gains
SYS	air conditioning system
T	temperature (°C)
ΔT	temperature difference (°C)
$\overline{T}$	average temperature (°C)
TCR	temperature change rate (°C/min)
t	time (s)
y_i	actual value
$\hat{y}_i$	predicted value
$\overline{y}_i$	average of the actual value
α	adjustment factor
τ	time constant

Subscripts

bui	building
i	step
in	indoor
j	step
out	outdoor
sys	air conditioning system

of demand-side flexibility resources (Liu et al. 2022; Zhang et al. 2024b). Public buildings, as essential components for grid flexibility, possess considerable potential in smart grid systems due to their significant energy consumption and passive thermal storage potential (Luo and Shi 2024; Zhu et al. 2025). Specifically, heating, ventilation, and air conditioning (HVAC) systems, which account for 40% to 60% of total energy consumption in buildings (Dai et al. 2023c, 2024), are key components in this regard. HVAC systems are well-suited for flexible control, with advantages such as ease of integration into existing energy management systems, low-cost implementation of flexible control (Sun et al. 2024), and the ability to maintain occupant comfort by leveraging thermal inertia. These characteristics make HVAC systems ideal resources for alleviating grid stress (Zhang and Kummert 2021).

In the context of modern demand response markets, particularly in day-ahead markets, there is a critical need to forecast/quantify flexibility in advance (Huang et al. 2025). Accurate quantification of demand-side flexibility allows the grid to plan ahead, enabling more effective unit commitment and economic dispatch, and ultimately ensuring system stability (Yu et al. 2023).

The flexibility quantification of building air conditioning systems is inherently tied to the control strategies employed. Broadly, these strategies can be categorized into end-side and source-side control. The former adjusts indoor temperature setpoints to reduce power demand (Hu et al. 2017), while the latter modifies the cooling capacity by directly shutting down the chiller or adjusting the chilled water supply temperature setpoint (Su and Norford 2015a, 2015b). Compared to the end-side control, the source-side control allows for more rapid adjustments in electricity consumption, thus meeting the requirements of the strict power market, such as the ancillary services market (Dai et al. 2023a, 2023b).

For end-side control, one method for quantifying flexibility involves calculating energy consumption differences when buildings operate at different indoor temperature setpoints (Ala et al. 2020; Yuan et al. 2021). Specifically, energy simulation software is used to determine the cooling load differential between these setpoints (e.g., 24 °C vs. 26 °C). This cooling load difference is subsequently converted into the energy consumption difference using the coefficient of performance (COP), which is typically interpreted as building flexibility. However, the calculated flexibility actually does not account for the thermal storage of the building. This method is more suited for power markets that require continuous energy consumption reductions throughout the day. However, in most existing power markets, buildings normally only need to reduce load during peak hours, which can be achieved by raising the indoor temperature setpoint only during these hours. This strategy can leverage the building's thermal storage, theoretically leading to higher flexibility. Existing research has also proposed relevant flexibility quantification methods for such circumstances.

For example, Yin et al. (2016) used EnergyPlus software to assess building flexibility by increasing the indoor temperature setpoint only during peak hours and calculating the difference between peak load and baseline load. Ding et al. (2024) introduced two indicators (power flexibility and energy consumption flexibility) to analyze building flexibility by adjusting the indoor temperature setpoint. Similarly, Ruan et al. (2023) examined the impact of preheating strategies on building flexibility in heating scenarios, focusing on the effects of indoor preheating temperatures (24 °C and 25 °C), preheating durations (20–180 minutes, with 20-minute intervals), and building structural parameters.

For source-side control (such as shutting down chillers or adjusting the chilled water supply temperature setpoint), the corresponding quantification method is different from that of end-side control, which is explained as follows. For end-side control, the power use can only be reduced to a certain value that maintains the upper limit of indoor temperature (e.g., 26 °C). However, for source-side control, the power use can technically be decreased to zero, unless the indoor temperature exceeds the upper limit (e.g., 26 °C) for a specified period (e.g., one hour) (Huang et al. 2021). Therefore, with a limited demand response period, source-side control theoretically can provide greater flexibility. Based on this fact, a different quantification method is needed for source-side control. Currently, the quantification method related to source-side control is limited. Zhu et al. (2022) simulated a demand response event by shutting down all chiller plant equipment and quantified flexibility using several key metrics: maximum DR duration (s), maximum power reduction (kW), average power reduction (kW), and maximum power rebound (kW). Han et al. (2024) proposed an analytical method for flexibility quantification based on a 2R2C model. This approach eliminates the need for time-consuming numerical simulations, making it particularly suitable for building cluster applications.

However, existing studies still face several limitations. First, conventional flexibility quantification methods often provide only a single value to represent the flexibility of building HVAC systems (Li et al. 2019). In practice, users can choose different levels of power reduction (such as turning off varying numbers of chillers or adjusting the chilled water setpoint to different degrees), which results in different flexibility outcomes. Therefore, this study proposes a power reduction-duration curve rather than a specific value to quantify the flexibility. In addition, existing flexibility quantification methods predominantly focus on grid requirements. In practice, the corresponding thermal comfort cost (indoor temperature fluctuations) for consumers is also needed (Chen et al. 2018). This allows building managers to select the level of flexibility they can offer based on the cost they are willing to bear. To address this, this study proposes temperature variation curves during the demand response process from the building's perspective.

Second, most existing flexibility quantification methods overlook the impact of uncertainties (Luo et al. 2023a). In fact, such uncertainties can lead to significant biases (Amadeh et al. 2022; Shen and Wang 2024). To address this limitation, this study systematically evaluates the influence of uncertainty on flexibility quantification. Specifically, it analyzes the effects of COP uncertainty and internal heat gain uncertainty. COP uncertainty arises from variations during adjustments of indoor temperature or chilled water supply temperature setpoints. Internal heat gain uncertainty mainly results from the random occupant schedules.

In the field of flexibility quantification, grey-box models, especially resistance-capacitance (RC) models, are widely used in building thermal dynamics modeling due to their simplicity and clear physical interpretation (De Rosa et al. 2014). A first-order RC model simplifies the building's thermal behavior by representing the entire thermal mass as a single capacitance. While computationally efficient, this simplification limits its effectiveness for flexibility quantification because it overlooks the distinction between the fast dynamics of indoor air and the slower responses of the building envelope (Chen et al. 2019). Second-order RC models address this by independently modeling indoor air and structural mass dynamics, thereby improving accuracy. To further enhance fidelity, higher-order models have been developed. For instance, 3R2C models are employed for wall segments and zone-level characterization (Braun and Chaturvedi 2002). Hybrid models, such as 3R2C-2R2C (Lin et al. 2024) configuration, capture whole-building dynamics. Even more detailed configurations, such as 6R4C (Gao et al. 2019) and 7R3C (Fux et al. 2014), offer a finer resolution of heat storage and release. However, these increasingly complex structures primarily focus on refining the thermal processes of the building itself and still fall short in capturing the inertia of HVAC systems, leading to potential inaccuracies in flexibility quantification. To address this gap, this study introduces an RC-Mapping model, which can precisely describe the dynamic interplay among the building, HVAC systems, and the indoor environment.

In addition, in the model parameter identification process, many existing studies omit to mention the initialization process of model state parameters (e.g., wall temperature) (Bacher and Madsen 2011; Bagheri et al. 2017), or they apply simplified rules that yield only rough estimates (Vivian et al. 2017). However, accurate initialization of model state parameters is critical for model parameter identification (Zhuang et al. 2018). Moreover, during flexibility quantification (especially in short-term demand response events lasting only a few hours), the impact of initialization becomes more significant, which has been

demonstrated in our experimental results. To address this, an Enumerate-Comparison Method is proposed to initialize the model state parameters.

In summary, this study has three contributions, as follows:

(1) This study proposes a power reduction-duration curve rather than a single value to quantify the flexibility, which can reflect scenario-dependent flexibility outcomes. Simultaneously, this study provides temperature variation curves in demand response events, which help building managers estimate the thermal cost of demand response.

(2) This study systematically investigates how uncertainties in key parameters, including the COP and internal heat gains, affect flexibility quantification. The findings can provide practical guidance for buildings to account for such uncertainties to improve the accuracy of flexibility quantification.

(3) This study proposes a new model (i.e., RC-Mapping model) for flexibility quantification, which captures not only the thermal characteristics of the building but also the thermal characteristics of air conditioning systems. Moreover, this study proposes an Enumerate-Comparison Method to initialize the model state parameters, which can enhance model identification accuracy, thus improving the accuracy of the flexibility quantification.

The structure of this study is organized as follows: Section 2 outlines the methodology. Section 3 describes the test platform and the test arrangement. Section 4 presents the result and discussion. Section 5 concludes the study.

2 Methodology

The research framework is illustrated in Figure 1, including three research steps: RC-Mapping model development,

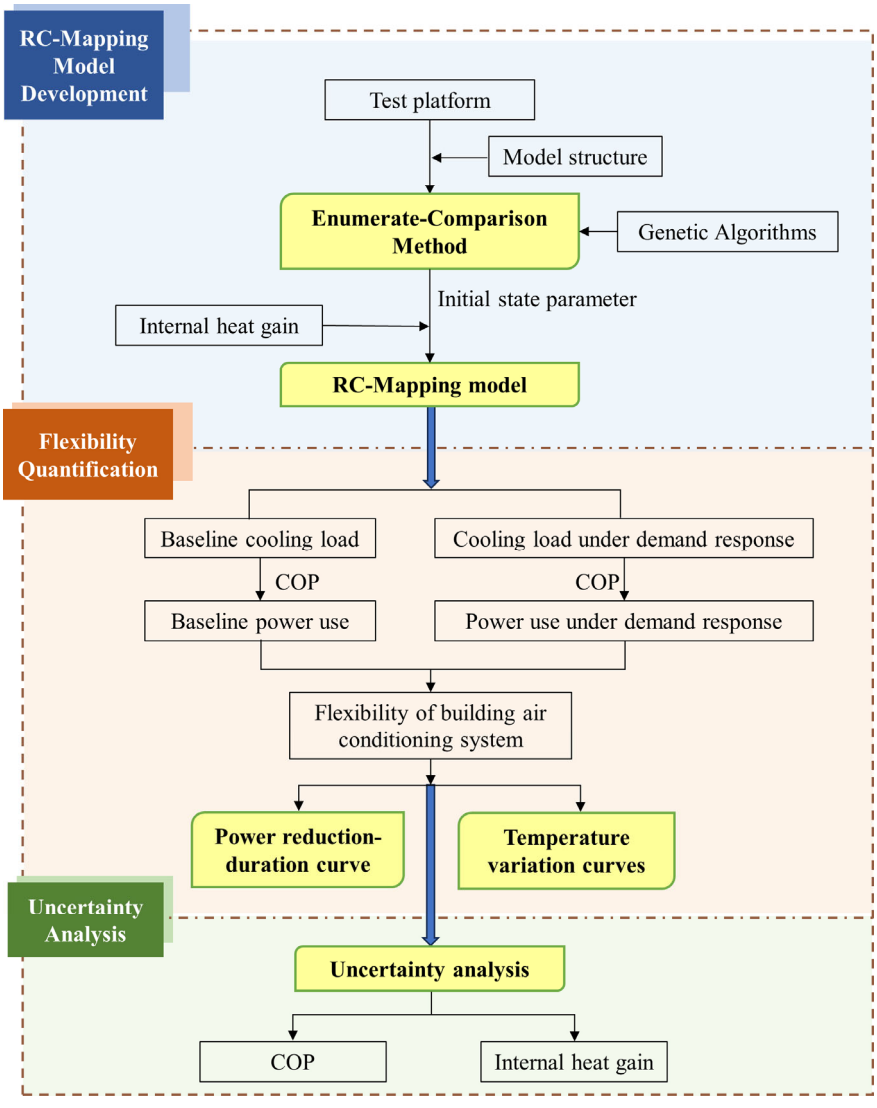

Fig. 1 Research framework

flexibility quantification, and uncertainty analysis. The yellow-highlighted boxes represent the study's key contributions, namely: the Enumerate-Comparison Method, the RC-Mapping model, the flexibility quantification curves, and the uncertainty analysis.

The three research steps are detailed as follows:

(1) RC-Mapping model development

The RC-Mapping model serves two key purposes: to predict the baseline power use and to predict the indoor temperature during demand response for flexibility quantification. Specifically, the Enumerate-Comparison Method is proposed to initialize state parameters. This research step is elaborated in Section 2.1.

(2) Flexibility quantification

Two curves are introduced for building flexibility quantification, as shown in Figure 2. The left curve is the reduction-duration curve. It shows how long different power reduction levels can be maintained before the indoor temperature rises from the baseline (e.g., 24 °C) to the upper comfort limit (e.g., 26 °C). The right curves are the indoor temperature variation curves, which describe the full indoor temperature response process during and after the demand response under various power reduction levels. This research step is elaborated in Section 2.2.

(3) Uncertainty analysis

An uncertainty analysis is conducted focusing on two primary sources that affect the flexibility quantification of building air conditioning systems, including COP and internal heat gain. The mean percentage error (MPE) is used to quantitatively evaluate the impact of parameter uncertainties on the flexibility quantification. This research step is elaborated in Section 2.3.

2.1 RC-Mapping model

2.1.1 *Model structure*

The proposed RC-Mapping model is illustrated in Figure 3. This model structure differs from conventional RC models in two primary ways: (1) the introduction of a novel RC model structure, and (2) a mapping model.

For the novel RC model structure, it can be observed that the cooling/heating supply of the air conditioning system (Q_{sys}) is connected to the temperature of the system (T_{sys}), which subsequently influences the indoor temperature (T_{in}) through a thermal resistance (R_{sys}). In contrast, conventional RC models connect Q_{sys} directly to T_{in} without accounting for the thermal dynamics of the air conditioning system itself. For the mapping model, the hour of the day (h) serves as an input to generate the corresponding internal heat gains, which are directly linked to T_{in}. The method for identifying internal heat gain schedules has been detailed in a separate publication by the author (Wang et al. 2025) and is therefore not elaborated here. To specifically assess the impact of schedule uncertainty on flexibility quantification, this study adopts schedule values from the national standard (MOHURD 2015), thereby ensuring a uniform and controlled basis for uncertainty analysis.

The mathematical description of the RC-Mapping model is shown as follows:

$$HT_1 = \frac{T_{in} - T_{sys}}{R_{sys}} \tag{1}$$

$$HT_2 = \frac{T_{wall} - T_{in}}{R_{bui,in}} \tag{2}$$

$$HT_3 = \frac{T_{out} - T_{wall}}{R_{bui,out}} \tag{3}$$

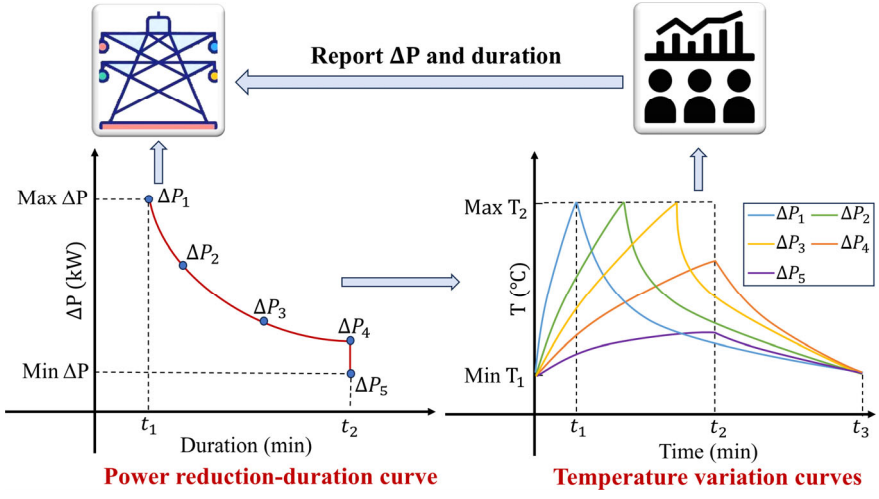

Fig. 2 Flexibility quantification

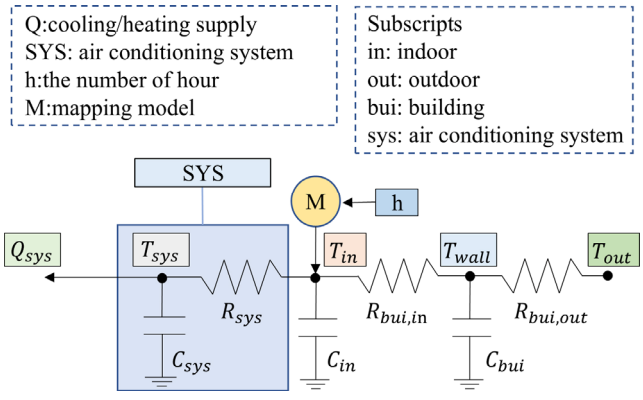

Fig. 3 RC-Mapping model

$$T_{\mathrm{sys},i+1} = \left(\mathrm{HT}_1 - Q_{\mathrm{sys}} \times \mathrm{ONOFF}\right) \times \frac{t}{C_{\mathrm{sys}}} + T_{\mathrm{sys},i} \tag{4}$$

$$T_{\mathrm{in},i+1} = \left(\mathrm{HT}_2 - \mathrm{HT}_1 + Q_{\mathrm{in}}\right) \times \frac{t}{C_{\mathrm{in}}} + T_{\mathrm{in},i} \tag{5}$$

$$T_{\mathrm{wall},i+1} = \left(\mathrm{HT}_3 - \mathrm{HT}_2\right) \times \frac{t}{C_{\mathrm{bui}}} + T_{\mathrm{wall},i} \tag{6}$$

$$Q_{\mathrm{in},h} = f(h) \tag{7}$$

where HT_1 indicates the heat transfer between indoor air and the air conditioning system; HT_2 indicates the heat transfer between the exterior envelope and indoor air; HT_3 indicates the heat transfer between outdoor air and the exterior envelope; T denotes the temperature; R is the thermal resistance; C is the thermal capacitance. The subscripts, *in, out, bui, sys,* and *i* indicate indoor, outdoor, building, air conditioning system and step. In this study, one step corresponds to one minute. Q_{sys} represents the cooling capacity supplied by air conditioning system; ONOFF denotes the operational status of the compressor, where an "on" state is indicated by 1 and "off" state by 0; t is the time, measured in seconds; h represents the hour of the day. Q_{in} is the internal heat gain. The equation $Q_{\mathrm{in}} = f(h)$ represents the Mapping model, which indicates the relationship between internal heat gains and the hour of the day. This relationship signifies that each specific hour uniquely corresponds to an internal heat gain value $Q_{\mathrm{in},h}$.

2.1.2 *Model identification*

The initialization of model state parameters directly affects the accuracy of parameter identification, thereby influencing the reliability of flexibility quantification. In the RC-Mapping model, the initial temperatures that need to be determined include the system temperature ($T_{\mathrm{sys},1}$), the indoor temperature ($T_{\mathrm{in},1}$), and the wall temperature ($T_{\mathrm{wall},1}$). Among these, $T_{\mathrm{in},1}$ can be directly assigned based on the measured indoor temperature. Given the air conditioning system is located indoors being off overnight, $T_{\mathrm{sys},1}$ is reasonably assumed to equal the indoor temperature.

However, accurately determining $T_{\mathrm{wall},1}$ poses significant challenges for two main reasons: (1) it would require sensors to be embedded within the wall, which is often impractical in real applications; and (2) in cases where the wall is represented using a multi-RC structure, there is no direct measurable physical temperature corresponding to the model state parameters in this structure. To address this limitation, this study proposes an Enumerate-Comparison Method for estimating the initial wall temperature. The overall process is illustrated in Figure 4, and the main steps are described as follows.

1) Define the assumed initial wall temperature $T_{\mathrm{wall},1}^{\mathrm{ass},j}$

Under normal conditions, the initial wall temperature $T_{\mathrm{wall},1}$ at a steady state typically lies between the indoor ($T_{\mathrm{in},1}$) and outdoor ($T_{\mathrm{out},1}$) temperatures. To explore this possibility range, a series of assumed initial wall temperatures $T_{\mathrm{wall},1}^{\mathrm{ass},j}$ is enumerated using the equation $T_{\mathrm{wall},1}^{\mathrm{ass},j} = T_{\mathrm{in},1} + j \times \alpha$, where j starts from 1, and α is a fixed adjustment factor. In this study, α is set to 0.1 °C. If there is a larger difference between the indoor and outdoor temperatures, a larger adjustment factor α can be chosen to accelerate the search process. In theory, the initial wall temperature may fall outside the indoor-outdoor range under rapid outdoor temperature fluctuations. However, such scenarios are not considered in this study. If needed, they can be accommodated by appropriately expanding the search range.

2) Identify the RC parameters corresponding to $T_{\mathrm{wall},1}^{\mathrm{ass},j}$

Each assumed value of the initial wall temperature is used to train the RC model based on data without internal heat gain using the genetic algorithm (GA). The objective function J_1 is defined as the root mean squared error (RMSE) between the predicted ($\hat{y}_i$) and actual (y_i) indoor temperatures:

$$\min J_1\left(R_{\mathrm{sys}}, C_{\mathrm{sys}}, R_{\mathrm{bui,in}}, C_{\mathrm{in}}, R_{\mathrm{bui,out}}, C_{\mathrm{bui}}\right) = \sqrt{\frac{1}{n}\sum_{i=1}^{n}\left(y_i - \hat{y}_i\right)^2} \tag{8}$$

3) Choose the optimal RC parameters

Due to the inherent randomness of the GA, for each assumed initial wall temperature, the RC parameters are trained W times. For each time, a group of RC parameters can be obtained. Then, it can calculate the total deviation (σ) of each group of RC parameters compared to the average RC parameters in W groups, as defined in Equation (9). The group with the minimum deviation is chosen as the optimal RC parameters set.

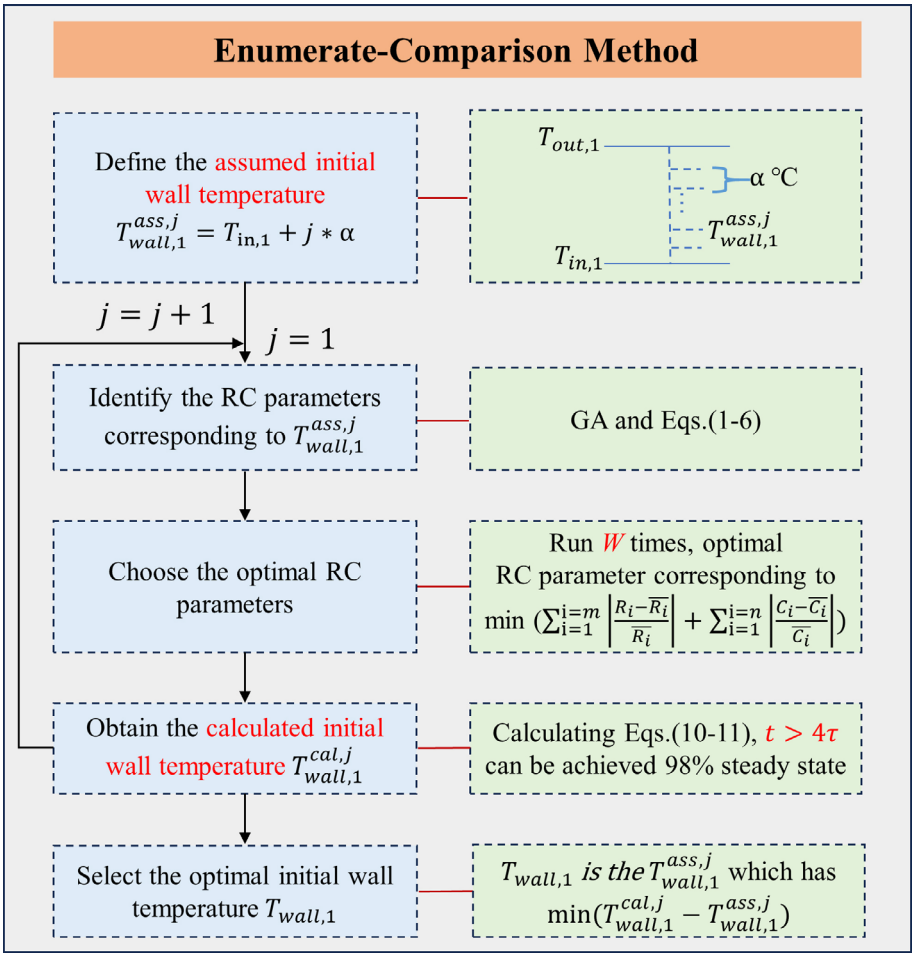

Fig. 4 Enumerate-Comparison Method

$$\sigma = \sum_{i=1}^{i=m} \left| \frac{R_i - \overline{R}_i}{\overline{R}_i} \right| + \sum_{i=1}^{i=n} \left| \frac{C_i - \overline{C}_i}{\overline{C}_i} \right| \tag{9}$$

The model follows an mRnC structure, where m and n represent the number of thermal resistances and thermal capacitances, respectively. In this study, a 3R3C model is adopted, so m = 3 and n = 3. And $R_1 = R_{sys}$, $R_2 = R_{bui,in}$, $R_3 = R_{bui,out}$, $C_1 = C_{sys}$, $C_2 = C_{in}$, $C_3 = C_{bui}$, $\overline{R}_i$, $\overline{C}_i$ are the average values of R_i and C_i in W groups of training.

4) Obtain the calculated initial wall temperature $T_{wall,1}^{cal,j}$

After choosing the optimal RC parameters, the calculated initial wall temperature can be obtained using historical variables (T_{in}, T_{out}) based on Equation (10).

$$C_{bui} \cdot \frac{dT_{wall}}{dt} = \frac{T_{in} - T_{wall}}{R_{bui,i}} + \frac{T_{out} - T_{wall}}{R_{bui,o}} \tag{10}$$

Here, an important question needs to be answered: how far back do indoor and outdoor temperatures continue to influence the current wall temperature? According to Equation (10), the time constant τ is can be derived as:

$$\tau = \left(\frac{1}{R_{bui,i}} + \frac{1}{R_{bui,o}} \right)^{-1} \cdot C_{bui} \tag{11}$$

Based on the exponential decay behavior of first-order systems, the wall temperature reaches approximately 98% of its steady-state value after a period of 4τ. Therefore, the historical variables (T_{in}, T_{out}) within the 4τ time window should be used to obtain the calculated initial wall temperature ($T_{wall,1}^{cal,j}$) based on Equation (10).

5) Select the optimal initial wall temperature by comparing the assumed and calculated initial wall temperature

The calculated and assumed initial wall temperatures are compared ($T_{wall,1}^{cal,j}$ vs $T_{wall,1}^{ass,j}$), and the one ($T_{wall,1}^{ass,j}$) with the smallest absolute difference is chosen as the optimal initial wall temperature, $T_{wall,1}$.

Following Steps (1) to (5), the optimal initial wall temperature ($T_{wall,1}$) is identified. The RC parameters corresponding to this optimal temperature are selected as the optimal RC parameters.

2.2 Flexibility quantification

2.2.1 *Reduction-duration curve*

As mentioned above, the reduction-duration curve shows how long different power reduction levels can be maintained before the indoor temperature rises from the baseline (e.g., 24 °C) to the upper comfort limit (e.g., 26 °C).

The process begins with estimating the baseline power use, which represents the power required to maintain the baseline indoor temperature setpoint. This baseline is calculated using the RC-Mapping model and converted into power use based on the COP. Once the baseline is established, a series of power reduction scenarios are simulated by incrementally lowering the cooling supply. For each scenario, the RC-Mapping model is employed to predict the indoor temperature variation. The DR event is considered to end when the temperature reaches the upper comfort limit, and the time used is recorded as the duration corresponding to that power reduction level. Repeating this process across all candidate reduction levels yields a set of (power reduction, duration) pairs, which then generate the reduction-duration curve.

2.2.2 *Indoor temperature variation curves*

Indoor temperature variation curves show the indoor temperature changes during and after a demand response (DR) event across various power reduction levels. Generated by the RC-Mapping model, these curves have two phases: the temperature rise from the baseline (e.g., 24 °C) to the upper comfort limit (e.g., 26 °C) during DR, and the recovery phase where the temperature returns to baseline after cooling resumes.

To effectively capture the comfort cost that users may bear when adopting different levels of power reduction during a demand response event, two metrics are introduced: the average temperature during the demand response period ($\overline{T_{in}}$), and the temperature change rate (°C/min) which is defined in Equation (12).

$$\mathrm{TCR} = \frac{T_1 - T_2}{t_2 - t_1} \tag{12}$$

where T_1 and T_2 represent the indoor temperatures at the start and end of the demand response (DR) event, respectively; $t_2 - t_1$ denotes the duration of the DR event, measured in minutes.

2.3 Uncertainty analysis

In practical applications, even when the baseline cooling load is accurately estimated, uncertainties in key input parameters may still influence the results of flexibility quantification. Among these, two critical factors are the COP of the cooling system and the internal heat gains (Schedule). To evaluate the impact of parameter uncertainties, each parameter is independently perturbed within a specified range, while all other variables (e.g., baseline load) are held constant. The resulting effect on flexibility quantification is then assessed.

3 Test platform and test arrangement

This section provides details about the test platform, including the room and air conditioning system, the control system, and the specifications of devices. Following this, the test arrangement is introduced.

3.1 Test platform

The test platform, as shown in Figure 5, is established in a conference room. The room is north-facing, with a floor area of 30 square meters. It features a ducted air conditioning unit (fixed-frequency) with two air outlets and connecting air ducts.

The air conditioning system is controlled via Python scripts, which allow for setting the system's on/off status, temperature setpoints, and airflow rate (high, medium, low). Commands are sent using the Minimal Modbus library to an RS485 controller, which subsequently sends an infrared signal to the air conditioning control panel, as illustrated in Figure 6(a).

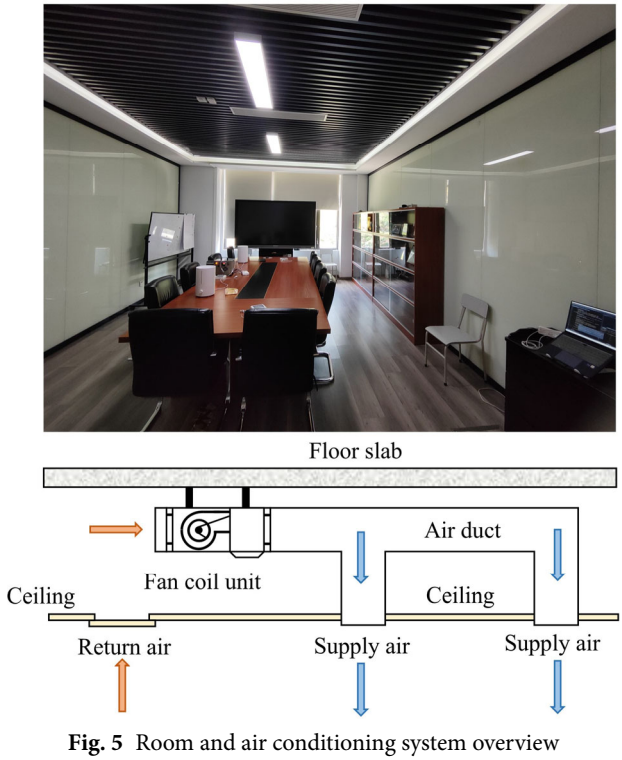

Fig. 5 Room and air conditioning system overview

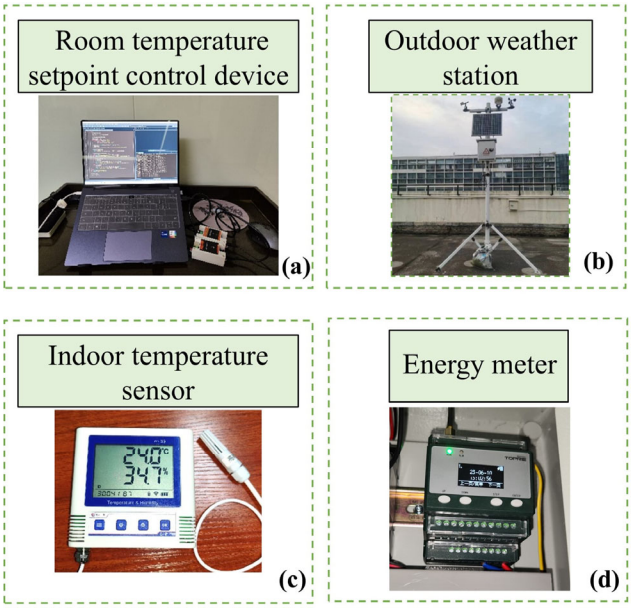

Fig. 6 Air conditioning system test setup

To construct the RC-Mapping model (as described in Section 2.1), three types of variables are required: outdoor temperature T_{out}, indoor temperature T_{in}, and cooling supply Q_{sys} from the air conditioning system. Outdoor temperature is measured using a weather station placed on the rooftop, as shown in Figure 6(b). Indoor temperature is obtained as the average from two sensors placed in different parts of the room, one of which is shown in Figure 6(c). The cooling supply is calculated by dividing the power consumption by the COP of the system. Power is measured by an energy meter, as shown in Figure 6(d). The COP, derived from the rated cooling capacity and power as provided by the manufacturer, is assumed constant throughout this study. Further details about the devices used are provided in Table 1. Data collection occurs every minute.

3.2 Test arrangement

In this study, four days are involved. Among them, the first three days are implemented through experiments, which are used for model development. Day 4 represents a standardized day, which is employed for flexibility quantification. The indoor and outdoor temperatures during these four days are shown in Figure 7. The details of each day are as follows.

- **Day 1:** The indoor temperature was maintained between 24 °C and 26 °C. To achieve this, the air conditioning was activated when the indoor temperature reached or exceeded 26 °C, and the compressor was turned off when the temperature dropped to 24 °C. It should be noted that the fan remained operational to fully leverage the system's thermal storage.
- **Day 2 and Day 3:** Similar to Day 1, the indoor temperature was maintained between 24 °C and 26 °C. However, the outdoor temperature on these days was higher, with a maximum outdoor temperature nearing 36 °C. These two days are selected to validate the model's performance during demand response events, which typically occur during periods of high outdoor temperatures.
- **Day 4:** Based on historical weather data, hourly outdoor temperature data from 15 consecutive days in July 2024 is selected. The average of these hourly values is used to construct a standardized outdoor temperature profile. To match the study's minute-level resolution, linear interpolation is applied to each hour, generating 59 intermediate values and yielding a smooth minute-by-minute temperature curve. The indoor temperature is set consistently at 24 °C.

According to the proposed methodology, the study procedure consists of three Setups, as detailed below.

- **Setup 1: RC-Mapping model development**

The model is trained using data from Day 1 and validated using data from Day 2 and Day 3. The model performance is evaluated from two perspectives: (1) the accuracy of indoor temperature prediction, and (2) the accuracy of flexibility quantification. Here, the flexibility is defined as the duration for the indoor temperature to rise from the baseline level (e.g., 24 °C) to the upper comfort limit (e.g., 26 °C) after the compressor shutdown. In addition, to evaluate the effectiveness of the proposed Enumerate-

Table 1 Detailed information on devices in the test platform

Name/type	Measured parameters	Measured accuracy	Measured range	Communication method
Room temperature setpoint control device	/	/	/	RS485
Weather station	Temperature	±0.1 °C	40 °C ± 80 °C	4G
Indoor temperature sensor	Temperature	±0.1 °C	40 °C ± 60 °C	Wi-Fi
Energy meter	Voltage	0.1%	0–480 V	4G
	Current	0.1%	0–20 A	
	Power	0.5%	0–9.6 kW	

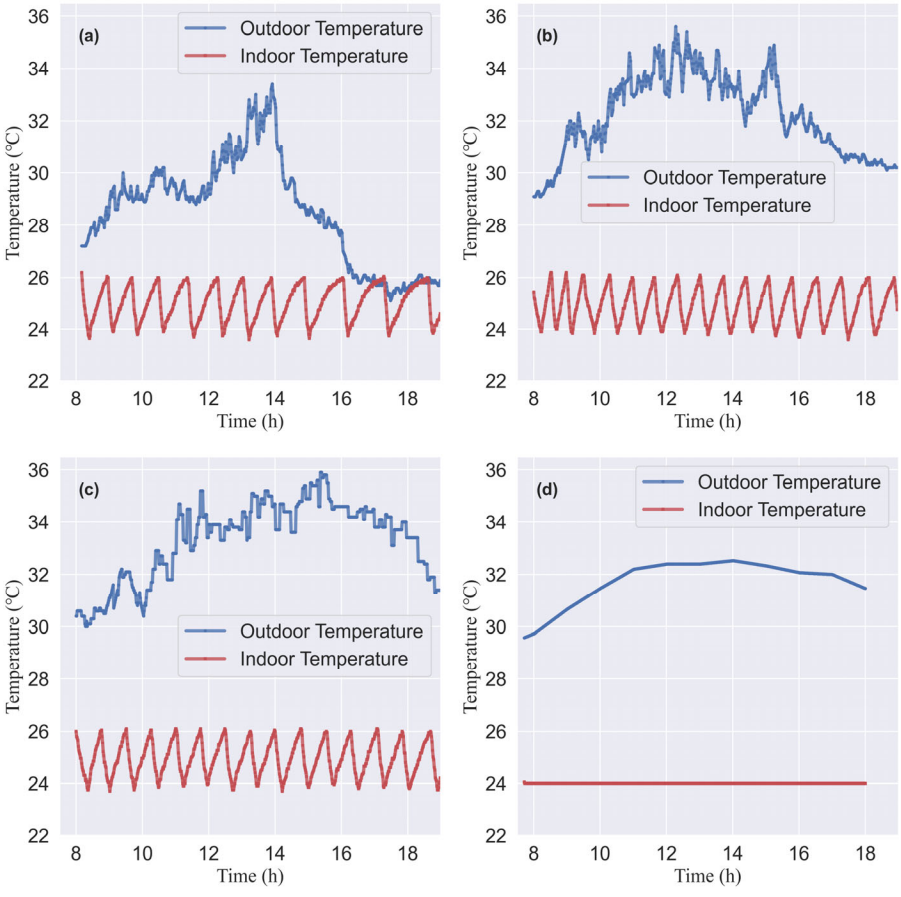

Fig. 7 The outdoor and indoor temperature of (a) Day 1, (b) Day 2, (c) Day 3, (d) Day 4

Comparison Method, which is used to determine the initial wall temperature $T_{wall,1}$. The model is also compared with a conventional approach where the initial wall temperature is set as the average of the initial indoor and outdoor temperatures. The results of this analysis are presented in Section 4.1.

- **Setup 2: flexibility quantification**

The hourly power reduction-duration curve is developed using data from Day 4. The baseline power is first calculated using the RC-Mapping model. Then, it is assumed that demand response strategies are applied at the beginning of each hour from 8:00 AM to 4:00 PM, covering a total duration of nine hours. For each hour, different levels of power reduction are implemented into the RC-Mapping model to obtain the duration for indoor temperature rise from 24 °C to 26 °C. According to the levels of power reduction and the corresponding duration, the power reduction-duration curve can be obtained. It should be noted that the power reduction levels started at 600 kJ/h (i.e., 166.67 W) and incrementally increased up to the baseline power level (i.e., the compressor turned off). Based on the power reduction-duration curves for each hour, a fundamental analysis is conducted on the sources of building flexibility. Additionally, the corresponding hourly indoor temperature variation curves are plotted and analyzed. The results of this analysis are presented in Section 4.2.

- **Setup 3: uncertainty analysis**

For this part, the COP and schedule are individually varied by ±10% and ±20%, respectively, under fixed conditions. Here, the uncertainty range is determined according to the chiller part-load performance curve and the prediction error of the internal heat gain schedule (Lin et al. 2024). Then, their impacts on flexibility quantification are analyzed. It should be noted that only 10:00 and 14:00 (peak hours) on Day 4 are selected as representative hours. The results of this uncertainty analysis are presented in Section 4.3.

4 Result and discussion

4.1 RC-Mapping model performance

4.1.1 Indoor temperature prediction performance

As mentioned in Section 3.2, the indoor temperature

prediction performance of the RC-Mapping model using the conventional method (i.e., $T_{wall,1} = 1/2(T_{in,1} + T_{out,1})$) is compared with that using the proposed Enumerate-Comparison Method. Figure 8(a) and Figure 8(b) show the validation results of the conventional method on Day 2 and Day 3, respectively, while Figure 8(c) and Figure 8(d) present the results of the Enumerate-Comparison Method on Day 2 and Day 3, respectively. In Figure 8, the green line represents the predicted indoor temperature, and the orange line represents the actual indoor temperature.

It can be observed that the RMSE decreased significantly when using the proposed method: from 0.616 °C to 0.283 °C on Day 2, and from 0.467 °C to 0.249 °C on Day 3, with an average decrease from 0.542 °C to 0.266 °C. These results demonstrate that the Enumerate-Comparison Method enables more accurate identification of the initial wall temperature, which significantly contributes to the enhanced predictive performance of the model.

4.1.2 *Flexibility quantification performance*

As mentioned in Section 3.2, the flexibility quantification performance of the RC-Mapping model using the conventional method is compared with that using the proposed Enumerate-Comparison Method. The duration for the indoor temperature to rise from 24 °C to 26 °C each time (on Day 2 and Day 3) is used to measure flexibility. Figure 9(a) and Figure 9(b) show the validation results of the conventional method on Day 2 and Day 3, respectively, while Figure 9(c) and Figure 9(d) present the results of the Enumerate-Comparison Method on Day 2 and Day 3, respectively.

As shown in Figure 9, the duration for the indoor temperature to rise from 24 °C to 26 °C exhibits an increasing trend. The main reason is that the air conditioning system was turned off the night before, resulting in a relatively high initial wall temperature ($T_{wall,1}$). During the subsequent operation phase, the indoor temperature was maintained between 24 °C and 26 °C, which progressively reduced $T_{wall,1}$. Although each stage started from the indoor temperature of 24 °C, the initial T_{wall} became lower in the later stages, leading to longer durations required for the indoor temperature to reach 26 °C.

According to the results, the mean absolute percentage error (MAPE) of the duration can be calculated. It can be found that the MAPE decreased from 32.72% to 11.48% on Day 2, and from 22.43% to 10.47% on Day 3, with an average decrease from 27.58% to 10.98%. These results further demonstrate that the Enumerate-Comparison Method allows for more accurate identification of the initial wall temperature, which in turn significantly enhances the model's performance in flexibility quantification.

The reasons why accurate identification of the initial wall temperature significantly enhances the precision of flexibility quantification are analyzed as follows. In practical applications, due to the substantial thermal capacity of buildings, the response time of wall temperature typically

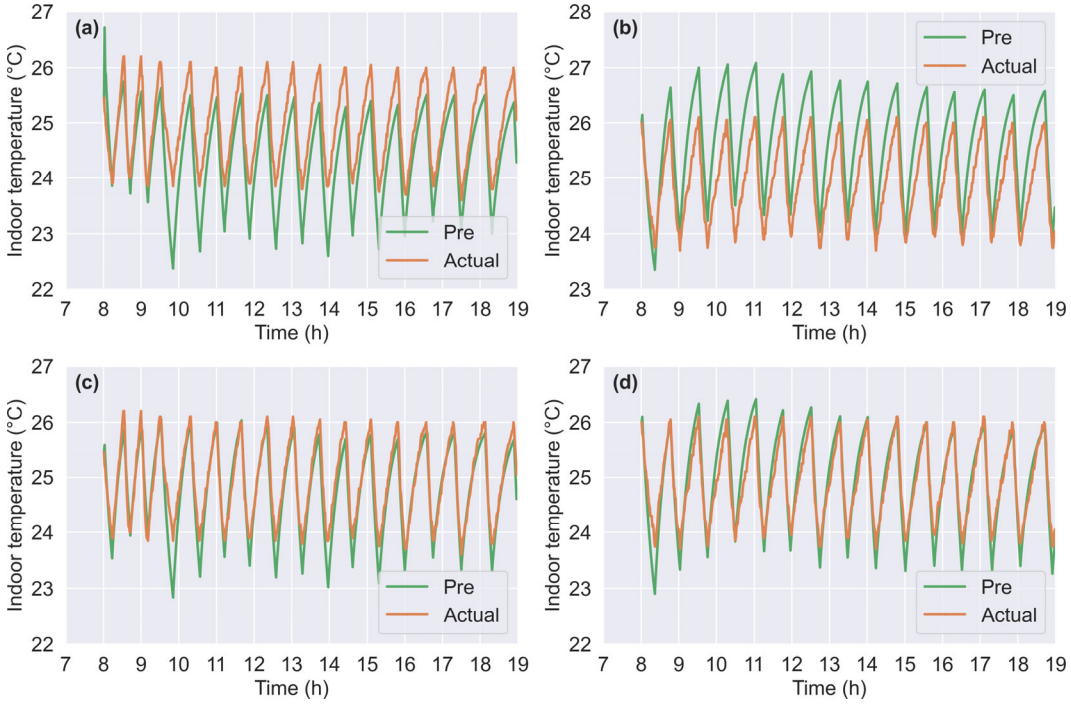

Fig. 8 Indoor temperature prediction performance of the conventional method on (a) Day 2 and (b) Day 3, and of the Enumerate-Comparison Method on (c) Day 2 and (d) Day 3

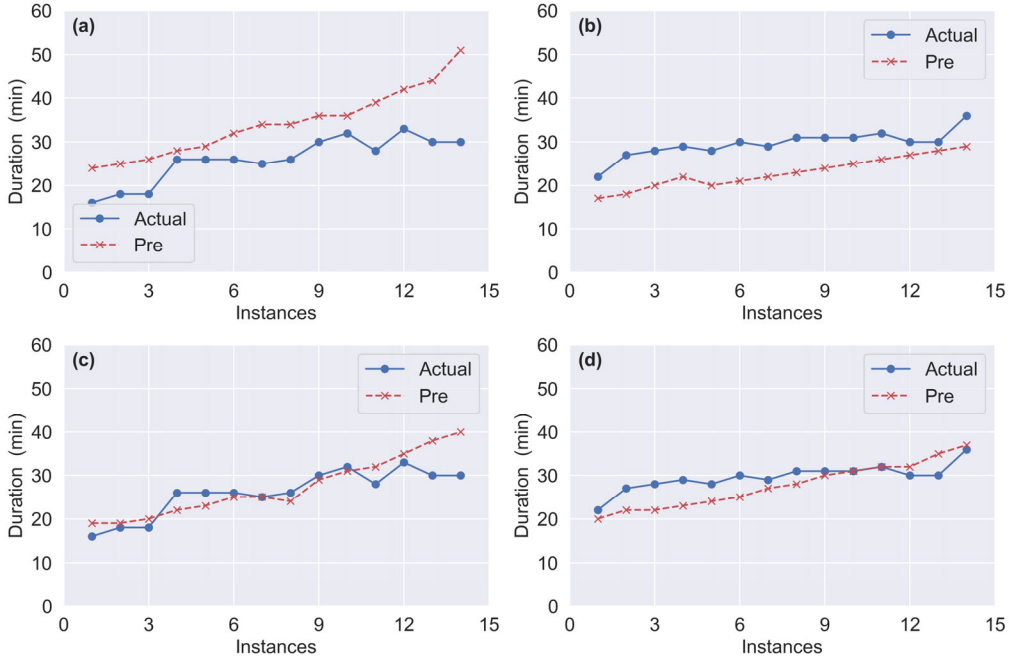

Fig. 9 Flexibility quantification performance of the conventional method on (a) Day 2 and (b) Day 3, and of the Enumerate-Comparison Method on (c) Day 2 and (d) Day 3

exceeds 10 hours. However, demand response events are relatively short, usually lasting only 1 to 2 hours. Therefore, if the initial wall temperature is not accurately estimated, it can remain inaccurate throughout the entire demand response period, introducing a persistent bias in indoor temperature prediction.

The proposed method effectively addresses the challenge of accurately determining the initial wall temperature, thereby enhancing flexibility quantification in both model development and application stages. In the model development stage, it facilitates the identification of more accurate model parameters. In the model application stage, a more accurate estimation of the initial wall temperature can contribute to improved quantification accuracy.

4.2 Hourly flexibility quantification

4.2.1 Power reduction-duration curve

Figure 10 shows the hourly power reduction-duration curves. The following observations can be drawn:

(1) Baseline power use determines the maximum power reduction (unit: W). The maximum reduction power for each hour is defined by the baseline power use, corresponding to the case when the air conditioning compressor is completely shut off.

(2) Under the same power reduction conditions, the duration remains consistent across different hours, even with changes in outdoor temperature. This result indicates that outdoor temperature does not impact the power reduction-duration relationship, although intuitively, higher outdoor temperatures would lead to shorter durations. The reason is that higher outdoor temperatures also correspond to higher baseline power use. As a result, when the same amount of power is reduced, the remaining power use is still higher than that under lower outdoor temperatures. Consequently, the rate of temperature increase remains the same, and thus, it does not affect the duration.

The flexibility quantification is calculated using Equation (13).

$$\text{flexibility quantification} = \Delta P \times \text{Duration} \tag{13}$$

As shown in Figure 10(a), there is a clear difference between Area X and Area Y ($Y > X$), indicating that the building exhibits different levels of flexibility under varying power reduction levels. To better explain this phenomenon, this study first provides a systematic analysis of the sources of flexibility and their underlying mechanisms. From the authors' perspective, building flexibility during demand response mainly originates from the following four sources.

(1) Thermal storage of the building: the building has a large thermal storage. When the air conditioning system is turned off or operates at reduced power, this stored energy helps slow down the rise in indoor temperature. Therefore, the thermal storage of the building is one of the core sources of flexibility.

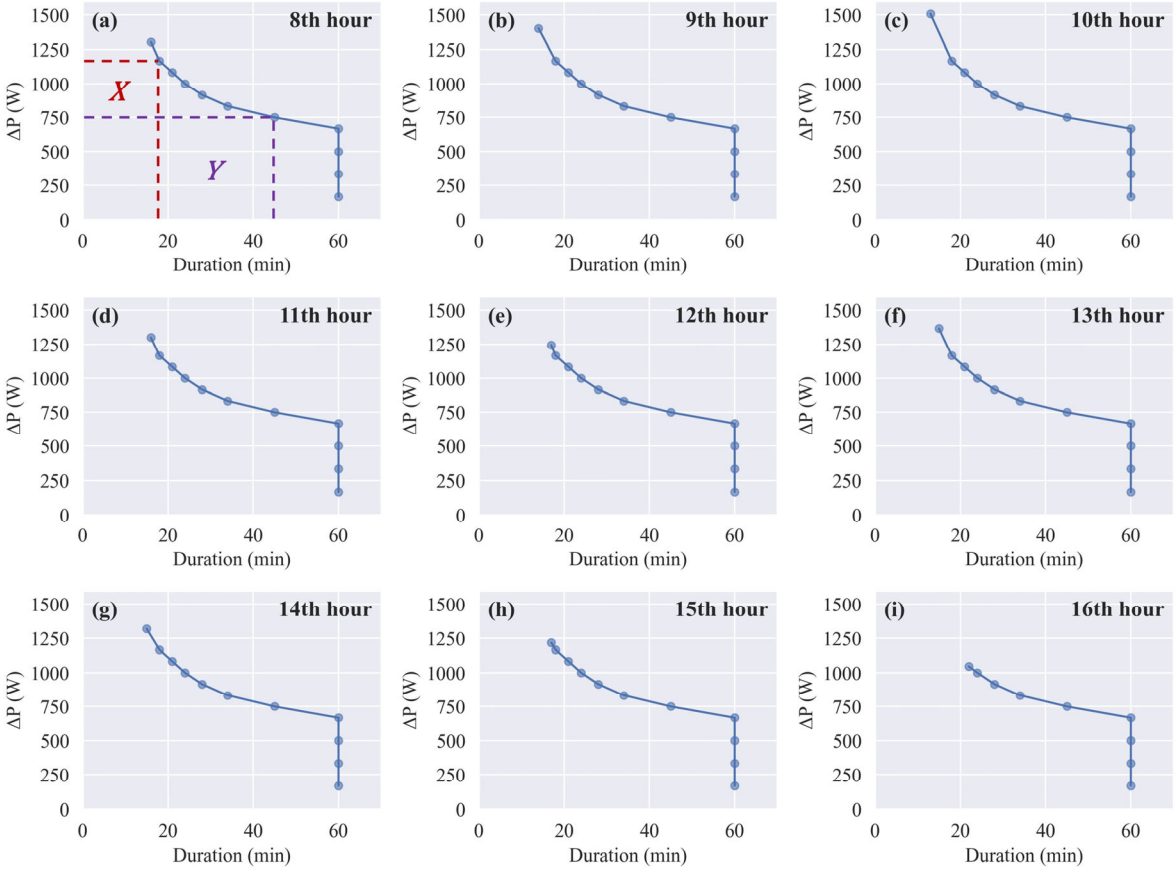

Fig. 10 Hourly power reduction-duration curve

(2) Thermal storage of the HVAC system: the HVAC system itself also has thermal storage capacity, including water systems, air systems, and air handling units. The cooling energy stored in the HVAC system can provide a non-negligible amount of flexibility during short-term demand response events.

(3) Increase in coefficient of performance (COP): during demand response, the evaporating temperature of the air conditioning system typically increases (e.g., increasing the chilled water supply temperature), leading to an increase in COP. A higher COP allows the system to deliver more cooling with the same power use, thereby extending the response duration. Thus, the increase in COP can be considered an indirect source of flexibility.

(4) Reduction in cooling load: as indoor temperature increases, the temperature difference between the indoor and outdoor environment decreases, which decreases the cooling load. This helps extend the duration for which the indoor temperature remains within the comfort range. Therefore, a reduction in cooling load is also considered an indirect source of flexibility.

Following the systematic analysis of the sources of flexibility, the reason for Area *Y* being larger than Area *X* can be explained as follows. First, the scenario corresponding to Area *Y* involves a smaller power reduction level, which naturally results in a longer duration. This extended duration allows the building and HVAC system to release more stored cooling energy. In turn, the additional released cooling further prolongs the duration, creating a positive feedback loop. Second, because the duration corresponding to Area *Y* is larger, the accumulated reduced cooling load is also larger, which can prolong the duration. To illustrate this mechanism, consider a hypothetical case: let *A* be the cooling load required to maintain 24 °C, and *B* the cooling load to maintain 26 °C. As long as the reduced cooling power remains less than or equal to the difference (*A*−*B*), the system can theoretically maintain the indoor temperature below 26 °C indefinitely, implying an infinite duration and, consequently, infinite flexibility. It is worth noting that the coefficient of performance (COP) is assumed constant in our case study and thus does not influence the comparative analysis.

4.2.2 *Indoor temperature variation curve*

Since the indoor temperature variation curves are similar across different hours, this study selects 10:00 and 14:00 as representative peak periods for detailed analysis. Figure 11 shows indoor temperature variation curves during and after

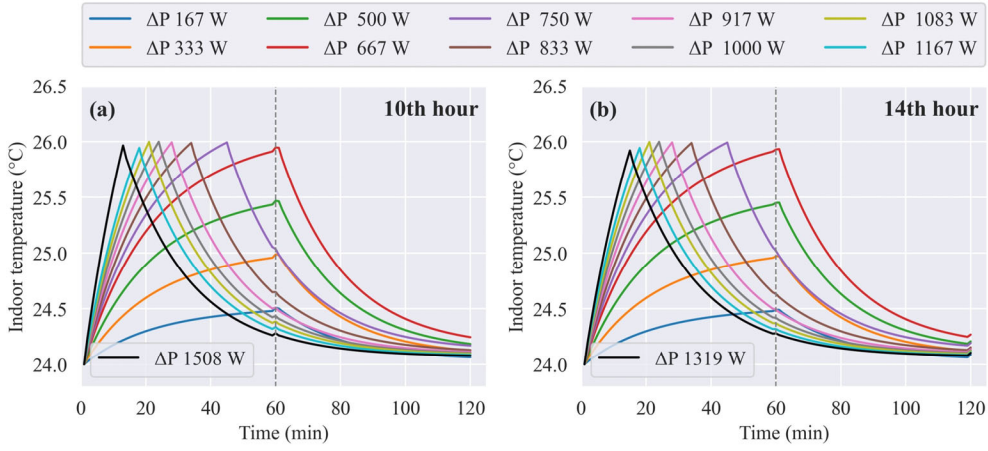

Fig. 11 Indoor temperature variation curves during and after the demand response at (a) 10:00 and (b) 14:00

the demand response at 10:00 and 14:00 under different power reduction levels.

As mentioned in Section 2.2.2, two metrics are used to quantify the thermal comfort cost: the average temperature during the demand response period ($\overline{T_{in}}$), and the temperature change rate (°C/min), which are calculated and presented in Figure 12 and Figure13, respectively.

Figure 12 shows the average temperature ($\overline{T_{in}}$) under different power reduction levels at 10:00 and 14:00. Through a combined analysis with Figure 10, it can be observed that the case with the highest average temperature (power reduction: 667 W) corresponds to the maximum flexibility. This indicates that the gain in flexibility is directly linked to the extent of comfort sacrifice. Occupants can determine their acceptable level of power reduction based on their acceptable comfort threshold.

Figure 13 shows the temperature change rate for different power reduction levels at 10:00 and 14:00. Even in the case of direct system shutdown, the observed temperature change rate (TCR) remained around 0.12 °C/min. This

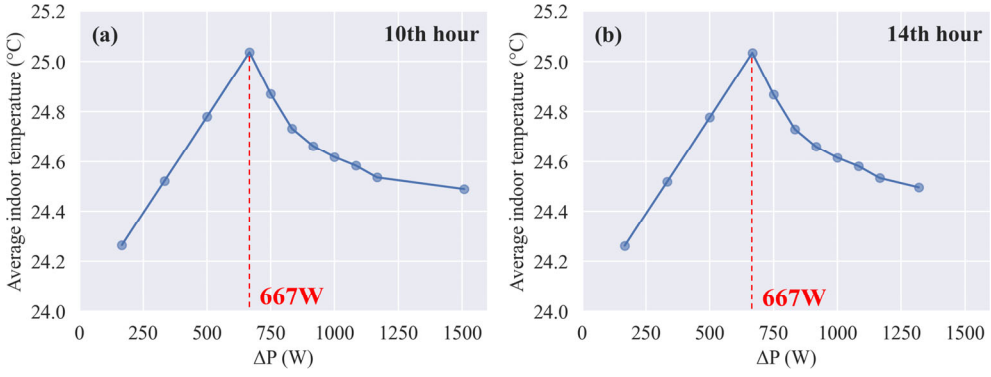

Fig. 12 The average indoor temperature under different power reduction levels at (a) 10:00 and (b) 14:00

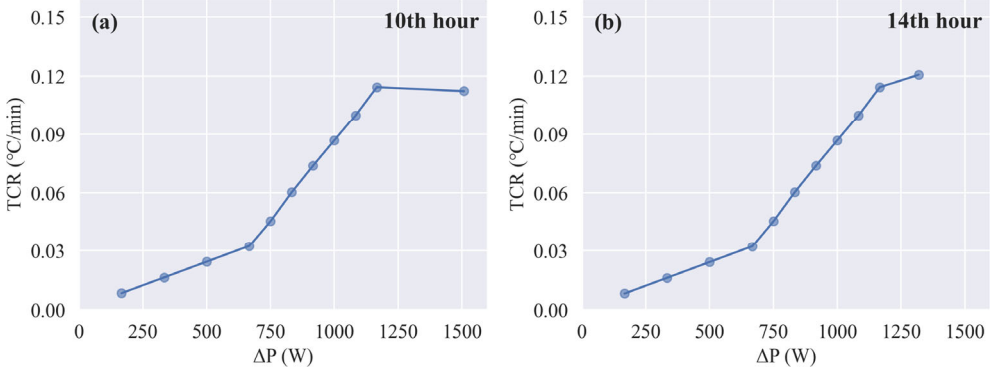

Fig. 13 The temperature change rate for different power reduction levels at (a) 10:00 and (b) 14:00

value is below the 0.15 °C/min threshold identified in Zhang et al. (2024a) as the upper limit for maintaining thermal comfort.

4.3 Uncertainty analysis

4.3.1 COP uncertainty analysis

Figure 14 shows the power reduction-duration curves under different COP values at (a) 10:00 and (b) 14:00.

It can be observed that with the same level of power reduction, the systems with higher COP can maintain a longer duration. To further quantitatively evaluate the impact of COP variation on flexibility quantification, this study employs the mean percentage error (MPE) as a performance indicator, as defined in Equation (14).

$$\mathrm{MPE} = \frac{1}{n}\sum_{i=1}^{n}\left(\frac{F_i - F_\mathrm{b}}{F_\mathrm{b}}\right)\times 100\% \tag{14}$$

where F_i represents the flexibility under different power reduction levels, and F_b refers to the flexibility for the baseline case.

Table 2 provides the MPE results for different COP deviations. It is important to note that overestimating the COP leads to greater estimation errors compared to underestimating it. The underlying reason is that a higher assumed COP implies a larger amount of cooling provided, which increases the estimated duration. Due to the positive feedback loop mentioned in Section 4.2.1 (explaining why Areas $Y > X$), the duration estimation error exhibits a power-like relationship with the final flexibility quantification result. For instance, with the same 10% deviation, 1.1 cubed equals 1.331 (a 33.1% error), while 0.9 cubed equals 0.729 (a 27.1% error). Therefore, overestimating the duration (i.e., overestimating the COP) tends to result in a larger flexibility quantification error.

In practical applications, although reducing power consumption (such as by increasing the chilled water supply temperature) can improve the COP, it is recommended to conservatively estimate the increase in the COP. On the one hand, this ensures more accurate flexibility quantification. On the other hand, it preserves a buffer to accommodate potential uncertainties during actual demand response, such as baseline load prediction errors and variations in occupancy.

4.3.2 Indoor heat gains (schedule) uncertainty analysis

Figure 15 shows the power reduction-duration curves under different schedule values at (a) 10:00 and (b) 14:00. Table 3 presents the corresponding MPE results. The results indicate that underestimating the indoor heat gain leads to greater estimation errors compared to overestimating it. The reason

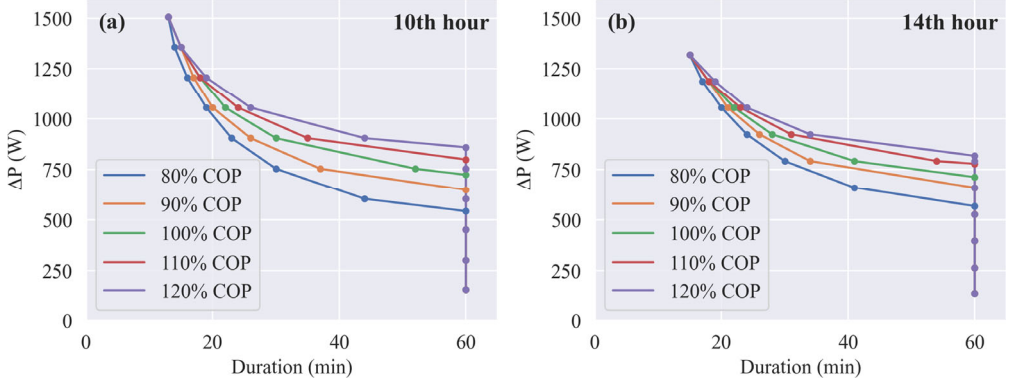

Fig. 14 Power reduction-duration curves under different COP deviations at (a) 10:00 and (b) 14:00

Table 2 MPE for different COP deviations

Hour	80% COP	90% COP	100% COP	110% COP	120% COP
10:00	−23.33%	−13.33%	0%	16.67%	46.67%
14:00	−14.29%	−7.14%	0%	10.71%	21.43%

Table 3 MPE for different schedule deviations

Hour	80% schedule	90% schedule	100% schedule	110% schedule	120% schedule
10:00	57.80%	19.40%	0%	−13.80%	−25.00%
14:00	48.50%	18.18%	0%	−15.15%	−24.24%

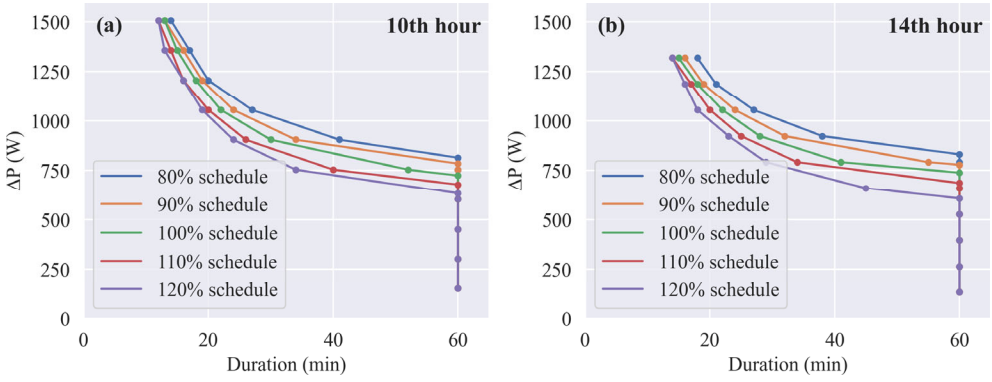

Fig. 15 Power reduction-duration curves under different schedule values at (a) 10:00 and (b) 14:00

is that underestimating the indoor heat gain can lead to overestimation of the duration. Because duration estimation error exhibits a power-like relationship with the final quantification result, as mentioned above. Overestimating the duration (i.e., underestimating the indoor heat gain) tends to result in a larger flexibility quantification error.

5 Conclusion

This study presents a systematic framework for the quantification of demand-side flexibility in building air conditioning systems, including RC-Mapping model development, flexibility quantification, and uncertainty analysis. The main conclusions are as follows:

- This study proposed a novel RC-Mapping model that integrates the Enumerate-Comparison Method, and exhibited excellent performance validated by experimental data. Compared with the conventional approach, it achieved substantial improvements in temperature prediction RMSE from 0.542 °C to 0.266 °C, and the MAPE for flexibility quantification from 27.58% to 10.98%.
- This study proposes two representative curves: the power reduction-duration curve and the temperature variation curves, which provide a comprehensive characterization of building flexibility from both the grid's and the end user's perspectives. Notably, the analysis reveals that outdoor temperature does not affect the reduction-duration curve.
- This study identifies four principal sources contributing to the flexibility of building air-conditioning systems: (1) the thermal storage of the building, (2) the thermal storage of the HVAC system, (3) the increase in COP, and (4) the reduction in cooling load.
- This study demonstrates that the COP and internal heat gains (Schedule) have a significant impact on flexibility quantification. For COP, overestimation tends to cause larger flexibility quantification deviations. For internal heat gains, underestimation tends to cause larger flexibility quantification deviations.

Acknowledgements

This study is funded by the National Natural Science Foundation of China (No. 52308104) and the Shenzhen Science and Technology Program (Grant No. KCXST20221021111203007).

Funding note: Open access publishing enabled by City University of Hong Kong Library's agreement with Springer Nature.

Declaration of competing interest

The authors have no competing interests to declare that are relevant to the content of this article. Yongjun Sun is an Editorial Board member of *Building Simulation*.

Author contribution statement

All authors contributed to the study conception and design. Material preparation was performed by Xiyin Weng. Data collection and analysis were performed by Huilong Wang and Yongjun Sun. The first draft of the manuscript was written by Xiyin Weng and Pengyuan Shen and all authors commented on previous versions of the manuscript. All authors read and approved the final manuscript.

References

Ala G, Di Gangi A, Zizzo G (2020). A methodology for evaluating the flexibility potential of domestic air-conditioning systems. In: Proceedings of 2020 IEEE 20th Mediterranean Electrotechnical Conference (MELECON), Palermo, Italy.

Amadeh A, Lee ZE, Zhang KM (2022). Quantifying demand flexibility of building energy systems under uncertainty. *Energy*, 246: 123291.

Arteconi A, Mugnini A, Polonara F (2019). Energy flexible buildings: A methodology for rating the flexibility performance of buildings with electric heating and cooling systems. *Applied Energy*, 251: 113387.

Bacher P, Madsen H (2011). Identifying suitable models for the heat dynamics of buildings. *Energy and Buildings*, 43: 1511–1522.

Bagheri A, Feldheim V, Thomas D, et al. (2017). The adjacent walls effects in simplified thermal model of buildings. *Energy Procedia*, 122: 619–624.

Braun JE, Chaturvedi N (2002). An inverse gray-box model for transient building load prediction. *HVAC&R Research*, 8: 73–99.

Chen Y, Xu P, Gu J, et al. (2018). Measures to improve energy demand flexibility in buildings for demand response (DR): A review. *Energy and Buildings*, 177: 125–139.

Chen Y, Chen Z, Xu P, et al. (2019). Quantification of electricity flexibility in demand response: Office building case study. *Energy*, 188: 116054.

Dai M, Li H, Wang S (2023a). Event-driven demand response control of air-conditioning to enable grid-responsive buildings. *Automation in Construction*, 150: 104815.

Dai M, Li H, Wang S (2023b). Multi-agent based distributed cooperative control of air-conditioning systems for building fast demand response. *Journal of Building Engineering*, 77: 107463.

Dai M, Li H, Wang S (2023c). Multi-agent based distributed cooperative control of air-conditioning systems for building fast demand response. *Journal of Building Engineering*, 77: 107463.

Dai M, Li H, Li X, et al. (2024). Reconfigurable supply-based feedback control for enhanced energy flexibility of air-conditioning systems facilitating grid-interactive buildings. *Advances in Applied Energy*, 14: 100176.

De Rosa M, Bianco V, Scarpa F, et al. (2014). Heating and cooling building energy demand evaluation; a simplified model and a modified degree days approach. *Applied Energy*, 128: 217–229.

Ding Y, Han S, Tian Z, et al. (2022). Review on occupancy detection and prediction in building simulation. *Building Simulation*, 15: 333–356.

Ding Y, Liu Y, Wang Q, et al. (2024). Flexibility potential quantification and regulation measure comparison for the building air-conditioning system. *Journal of Cleaner Production*, 434: 140086.

Fux SF, Ashouri A, Benz MJ, et al. (2014). EKF based self-adaptive thermal model for a passive house. *Energy and Buildings*, 68: 811–817.

Gao J, Yan T, Xu T, et al. (2019). Development and experiment validation of variable-resistance-variable-capacitance dynamic simplified thermal models for shape-stabilized phase change material slab. *Applied Thermal Engineering*, 146: 364–375.

Han B, Li H, Wang S (2024). A probabilistic model for real-time quantification of building energy flexibility. *Advances in Applied Energy*, 15: 100186.

Hu M, Xiao F, Wang L (2017). Investigation of demand response potentials of residential air conditioners in smart grids using grey-box room thermal model. *Applied Energy*, 207: 324–335.

Huang S, Ye Y, Wu D, et al. (2021). An assessment of power flexibility from commercial building cooling systems in the United States. *Energy*, 221: 119571.

Huang C, Li K, Zhang N (2025). Strategic joint bidding and pricing of load aggregators in day-ahead demand response market. *Applied Energy*, 377: 124552.

Klein K, Herkel S, Henning HM, et al. (2017). Load shifting using the heating and cooling system of an office building: Quantitative potential evaluation for different flexibility and storage options. *Applied Energy*, 203: 917–937.

Li K, Wang F, Mi Z, et al. (2019). Capacity and output power estimation approach of individual behind-the-meter distributed photovoltaic system for demand response baseline estimation. *Applied Energy*, 253: 113595.

Li R, Satchwell AJ, Finn D, et al. (2022). Ten questions concerning energy flexibility in buildings. *Building and Environment*, 223: 109461.

Lin X, Tian Z, Song W, et al. (2024). Grey-box modeling for thermal dynamics of buildings under the presence of unmeasured internal heat gains. *Energy and Buildings*, 314: 114229.

Liu J, Yin R, Yu L, et al. (2022). Defining and applying an electricity demand flexibility benchmarking metrics framework for grid-interactive efficient commercial buildings. *Advances in Applied Energy*, 8: 100107.

Luo Z, Peng J, Yin R (2023a). Many-objective day-ahead optimal scheduling of residential flexible loads integrated with stochastic occupant behavior models. *Applied Energy*, 347: 121348.

Luo Z, Peng J, Hu M, et al. (2023b). Multi-objective optimal dispatch of household flexible loads based on their real-life operating characteristics and energy-related occupant behavior. *Building Simulation*, 16: 2005–2025.

Luo X, Shi W (2024). Optimal regulation of flexible loads in rural residential buildings considering mobile batteries: A case study in Shaanxi Province. *Building Simulation*, 17: 1065–1083.

MOHURD (2015). GB 50189-2015: Design standard for energy efficiency of public buildings. Ministry of Housing and Urban-Rural Development of China. (in Chinese)

Rao Z, Chen S, Lun I, et al. (2023). Energy flexibility characteristics of centralized hot water system in university dormitories. *Building Simulation*, 16: 641–662.

Ruan Y, Ma J, Meng H, et al. (2023). Potential quantification and impact factors analysis of energy flexibility in residential buildings with preheating control strategies. *Journal of Building Engineering*, 78: 107657.

Shen P, Wang H (2024). Archetype building energy modeling approaches and applications: A review. *Renewable and Sustainable Energy Reviews*, 199: 114478.

Su L, Norford LK (2015a). Demonstration of HVAC chiller control for power grid frequency regulation: Part 1: Controller development and experimental results. *Science and Technology for the Built Environment*, 21: 1134–1142.

Su L, Norford LK (2015b). Demonstration of HVAC chiller control for power grid frequency regulation: Part 2: Discussion of results and considerations for broader deployment. *Science and Technology for the Built Environment*, 21: 1143–1153.

Sun Y, Zhao T, Lyu S (2024). Model-based investigation on building thermal mass utilization and flexibility enhancement of air conditioning loads. *Building Simulation*, 17: 1289–1308.

Vivian J, Zarrella A, Emmi G, et al. (2017). An evaluation of the suitability of lumped-capacitance models in calculating energy needs and thermal behaviour of buildings. *Energy and Buildings*, 150: 447–465.

Wang H, Chen Y, Kang J, et al. (2023). An XGBoost-Based predictive control strategy for HVAC systems in providing day-ahead demand response. *Building and Environment*, 238: 110350.

Wang H, Weng X, Ji Y, et al. (2025). A novel RC-mapping model of building air conditioning systems dedicated to demand response and training condition analysis. *Journal of Building Engineering*, 108: 112774.

Yin R, Kara EC, Li Y, et al. (2016). Quantifying flexibility of commercial and residential loads for demand response using setpoint changes. *Applied Energy*, 177: 149–164.

Yu H, Zhong F, Du Y, et al. (2023). Short-term cooling and heating loads forecasting of building district energy system based on data-driven models. *Energy and Buildings*, 298: 113513.

Yuan J, Xiao Z, Chen X, et al. (2021). A temperature & humidity setback demand response strategy for HVAC systems. *Sustainable Cities and Society*, 75: 103393.

Zhang K, Kummert M (2021). Evaluating the impact of thermostat control strategies on the energy flexibility of residential buildings for space heating. *Building Simulation*, 14: 1439–1452.

Zhang X, Wang D, Wang W (2024a). Experimental analysis on flexible characteristics of air conditioning energy use in office buildings based on indoor set temperature regulation. *HV&AC*, *54*(10): 18–26. (in Chinese)

Zhang X, Xiao F, Li Y, et al. (2024b). Flexible coupling and grid-responsive scheduling assessments of distributed energy resources within existing zero energy houses. *Journal of Building Engineering*, 87: 109047.

Zhu J, Niu J, Tian Z, et al. (2022). Rapid quantification of demand response potential of building HAVC system *via* data-driven model. *Applied Energy*, 325: 119796.

Zhu J, Tian Z, Niu J, et al. (2025). Machine learning-enhanced lightweight rule-based control strategy for building energy demand response. *Building Simulation*, 18: 1857–1876.

Zhuang J, Chen Y, Chen X (2018). A new simplified modeling method for model predictive control in a medium-sized commercial building: A case study. *Building and Environment*, 127: 1–12.